doi:10.3772/j.issn.1006-6748.2020.02.006

Research on optimization design method of actuator parameters with stepless capacity control system for reciprocating compressor①

Zhou Chao(周 超)*, Zhang Jinjie②*, Sun Xu**, Wang Yao***

(* Compressor Health and Intelligent Monitoring Center of National Key Laboratory of Compressor Technology, Beijing University of Chemical Technology, Beijing 100029, P. R. China)

(** State Key Laboratory of Compressor Technology, Anhui Provincial Laboratory of Compressor Technology, Hefei 230031, P. R. China)

(*** Beijing Key Laboratory of Health Monitoring Control and Fault Self-Recovery for High-End Machinery, Beijing University of Chemical Technology, Beijing 100029, P. R. China)

Abstract

Actuator and hydraulic system parameters have great influence on the performance, safety and reliability of the stepless capacity control system of reciprocating compressor. Due to the diversity and complex relationship of parameters, traditional parameters selected and calculated based on feasibility can't make the system run efficiently, have limitations, and may have adverse effects on the system or compressor. Therefore, taking the spring stiffness of the actuator and the impact velocity of ejection, the inlet oil pressure of the hydraulic system, and the indicated power deviation of the compressor as objective functions, the multi-parameter and multi-objective optimization research of the actuator and hydraulic system with the stepless capacity control system based on non-dominated sorting genetic algorithm II (NSGA-II) is carried out. Based on fuzzy analytic hierarchy process (FAHP), the optimal solution is selected from the Pareto front, and compared with the traditional design value, the result is better than that obtained by the traditional design method.

Key words: reciprocating compressor, stepless capacity control system, non-dominated sorting genetic algorithm II (NSGA-II), fuzzy analytic hierarchy process (FAHP)

0 Introduction

In petroleum and chemical enterprises, many chemical or physical processes require high-pressure gases, and reciprocating compressors play an irreplaceable role because of their outstanding advantages in compression efficiency and compression ratio. Reciprocating compressor belongs to positive displacement compressor, the discharge is constant under normal working conditions, but the fluctuation of technological process makes the device not run at full load. Reciprocating compressor usually runs below the designed discharge, so it is usually equipped with capacity control system to meet the operating requirements. The capacity regulation by pressing-off suction valve during partial stroke can realize 0 – 100% stepless flow regulation theoretically by controlling the opening time of the unloading device in the compression process. At the same time, it also reduces energy consumption[1]. The capacity control system is installed on reciprocating compressor in a petrochemical refinery. When the load is 40% – 60%, the power can be saved by 300 kW/h. Calculated at 0.5 yuan/kWh, running for one year (that is 8 000 h) can save about 1.2 million yuan of electricity, with obvious energy-saving effect.

When the reciprocating compressor is installed with the stepless capacity control system[2-5], the actuator, control hardware and hydraulic system often fail because the design or control parameters are not optimized according to the actual situation in the field. The failure of hydraulic system is involved in Ref. [6]. The failure of control system is involved in Ref. [7]. The failure of actuator is involved in Refs[8-12]. Due to application problems, researchers begin to avoid problems in structure and parameter design. Wu et al.[13] analyzed the influence of inlet oil pressure on valve plate movement based on the mathematical model of valve plate movement and designed the optimal inlet

① Supported by the State Key Laboratory of Compressor Technology Open Fund Project (No. SKL-YSJ201808), the National Key Research and Development Plan (No. 2016YFF0203305) and the Special Fund Support for Basic Scientific Research Business Expenses of Central Universities (No. JD1912).

② To whom correspondence should be addressed. E-mail: zjj87427@163.com

Received on Sep. 2, 2019

oil pressure. Meanwhile, the speed buffer structure is designed to greatly reduce the impact of valve plate on valve seat and extend the life of valve plate. Li et al. [14] established a streamlined valve model and studied the relationship between inlet oil pressure and tilt angle and valve plate life, which provided theoretical basis for optimal design of actuator. Cao et al. [15] studied characteristics of hydraulic actuator and system modeling based on AMESim, and proposed an improved design. Li et al. [16] deduced an accurate calculation formula of discharge, and designed the GUI, which can quickly complete the design of the force of ejection. In conclusion, the researchers set single optimization goal and didn't consider the diversity of parameters which have complex relationship of mutual dependence and contradiction, so, the design results have limitations, which can not make the system in an efficient operation state.

The objectives are mutually restricted, and there are multiple groups of non-dominant solutions. Traditional multi-objective optimization methods can not be used to solve the above problems. The evolutionary multi-objective optimization method has achieved good results in practical application, and researchers have achieved rich research results. The non-dominated sorting genetic algorithm II (NSGA-II) [17,18] is currently one of the most popular multi-objective genetic algorithm (GA), which reduces the complexity of non-inferior sort genetic algorithm, and has the advantages of fast running speed and good convergence of solution set, and becomes the benchmark of other multi-objective optimization algorithms.

In this paper, mathematical models of actuators and compressors are established. According to the mutual influence relationship and importance of parameters, the indicated power deviation, impact velocity of ejection, inlet oil pressure and spring stiffness are selected as objective functions. The Pareto frontier is obtained by NSGA-II. Finally, the optimal solution is selected by fuzzy analytic hierarchy process and compared with the traditional design value. The result obtained is significantly better than that obtained by the traditional design method, which verifies the feasibility and effectiveness of the method.

1 Stepless capacity control system and mathematical model

The stepless capacity control system principle of reciprocating compressor is shown in Fig. 1. Under normal conditions, when the piston moves to the position of inner dead point (point A), it starts to reverse movement, the suction valve begins to close, and then the compressor compresses and exhausts. The area of the P-V diagram contains regions I and II. When the piston moves to the position of inner dead point (point A), it starts to move in the opposite direction. The hydraulic system provides a large hydraulic driving force to the unloader. The suction valve is forced to be pushed open by the unloader. The valve plate is at the lower limit and the gas returns to the suction chamber. When the piston moves to point B, the volume meets the production requirements. The hydraulic system provides the hydraulic driving force of the unloader to reduce, the spring force in the unloader overcomes the hydraulic driving force and friction, the unloader retracts, and the suction valve begins to close. The area of the P-V diagram contains region II. According to the area in the P-V diagram, the capacity control system can not only make the reciprocating compressor meet the volume requirements, but also save energy in region I. Nomenclature is listed in Table 1.

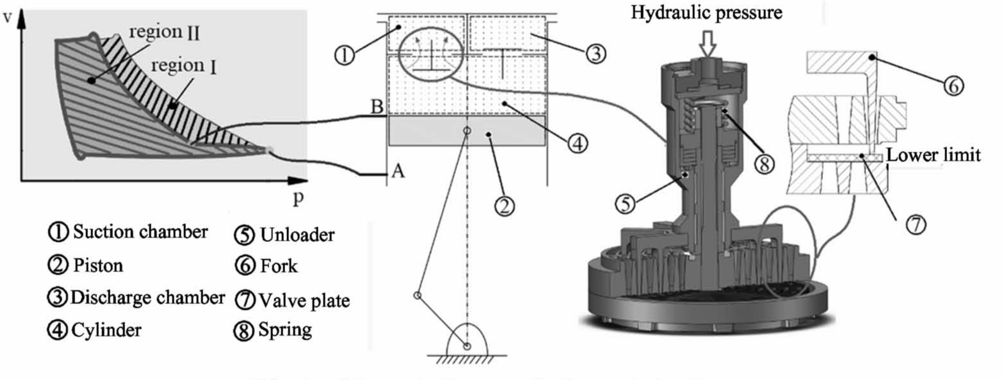

Fig. 1 Schematic diagram of valve and chamber

1.1 Mathematical model of actuator

The actuator is mainly composed of hydraulic cylinder, unloader including reset spring, executing fork, mandril and other components. The hydraulic system includes hydraulic stations and pipelines to provide the

Table 1 Nomenclature

Symbol	Name	Unit	Symbol	Name	Unit
F_h	Hydraulic driving force	N	θ_1	Start angle of ejection	°
p_1	Hydraulic driving force of ejection	Pa	θ_{s1}	Initial opening angle of suction valve plate	°
p_2	Hydraulic driving force with drawal	Pa	θ_2	End angle of ejection	°
A_{unloader}	Transversal area of hydraulic piston	m^2	θ_{s2}	Full opening angle of suction valve plate	°
F_i	Gas force of suction	N	θ_3	Start angle of withdrawal	°
F_s	Spring force of actuator	N	θ_{s3}	Normal condition initial closing angle of suction valve plate	°
F_{cy}	Gas force of cylinder	N	θ_4	End angle of withdrawal	°
γ	Gas force coefficient of valve plate		θ_{s4}	Normal condition full closing angle of suction valve plate	°
v_a	Actuator speed	$\text{m} \cdot \text{s}^{-1}$	θ_{s5}	Capacity regulation condition full closing angle of suction valve plate	°
x_0	Pre-compression	m	θ_{unloader}	Crank angle of withdrawal	°
L	Actuator trip	m	w	Angular velocity	rad/s
x	Actuator displacement	m	α	Installation angle of actuator	°
m	Actuator mass	kg	g	Gravitational acceleration	m/s^2
k_{unloader}	Spring stiffness of actuator	$\text{N} \cdot \text{m}^{-1}$	f	Total friction of actuator	N

driving force for the actuator to overcome the spring force, gas force, friction force, etc. The suction valve is delayed in closing from open state. Part of the gas returns to the suction chamber in compression stroke to realize the purpose of capacity control.

In order to analyze the motion characteristics of the actuator with stepless capacity control system, several hypotheses are provided.

(1) Don't consider the rebound of actuator during impact.

(2) Don't consider time delay of hydraulic system oil supply or unloading, that is, the start time of ejection or withdrawal of the loader is consistent with the start time of oil supply or unloading in the hydraulic oil unit.

i) Hydraulic driving force

$$F_h = \begin{cases} p_1 A_{\text{unloader}} & \theta_1 \leqslant \theta \leqslant \theta_2 \\ p_2 A_{\text{unloader}} & \theta_3 \leqslant \theta \leqslant \theta_4 \end{cases} \tag{1}$$

where, F_h represents the hydraulic driving force, p_1 represents the oil pressure in the ejection process of the actuator, p_2 represents oil pressure in the withdrawal process of the actuator, A_{unloader} represents transversal area of hydraulic piston, θ_1 represents start angle of ejection, θ_2 represents end angle of ejection, θ_3 represents start angle of withdrawal, θ_4 represents end angle of withdrawal.

ii) Spring force of actuator

$$F_s = k_{\text{unloader}}(x_0 + x) \tag{2}$$

where, F_s represents spring force of actuator, k_{unloader} represents spring stiffness of actuator, x_0 represents pre-compression, x represents actuator displacement.

iii) Differential equations of motion of ejection and withdrawal

$$m\frac{\mathrm{d}^2 x}{\mathrm{d}t^2} = \begin{cases} F_h - F_i + mg\cos\alpha - f - F_s & \theta_1 \leqslant \theta \leqslant \theta_2 \\ F_s - F_h - P + F_i - mg\cos\alpha + \gamma F_{cy} & \theta_3 \leqslant \theta \leqslant \theta_4 \end{cases} \tag{3}$$

where, m represents actuatormass, F_i represents gasforce of suction, α represents installation angle of actuator, f represents total friction of actuator, F_{cy} represents gas force of cylinder, γ represents gas force coefficient of valve plate, when executing fork contacts the valve plate, $\gamma = 1$, instead, $\gamma = 0$.

iv) Initial condition

$$\begin{cases} \left.\begin{matrix} v_a(0) = 0 \\ x(0) = x_0 \end{matrix}\right] & \theta_1 \leqslant \theta \leqslant \theta_2 \\ \left.\begin{matrix} v_a(0) = 0 \\ x(0) = x_0 + L \end{matrix}\right] & \theta_3 \leqslant \theta \leqslant \theta_4 \end{cases}$$

where, $x'(0)$ represents initial velocity in ejection or withdrawal of actuator, $v_a(0)$ represents initial displacement in ejection or withdrawal of actuator, L represents actuatortrip.

1.2 Mathematical model of compressor with stepless capacity control system

As shown in Fig. 2 and Table 2, on account of changing opening and closing states by actuator under capacity control condition, many new processes are added compared with the compressor model under normal working conditions. As shown in Fig. 2, the suction valve is forced open during compression stroke (crank angle is $\theta_{s3} - \theta_3$). The movement state of valve plate is changed. In the closing process of suction valve, if the acceleration of the unloader is less than the suction valve plate acceleration (crank angle is $\theta_{s5} - \theta_4$), the motion state of the valve plate closing process will also change.

Table 2 Description of unloader and suction valve

Angle	Yes or No / New process	Description
$\theta_{s1} - \theta_{s2}$	No	Capacity regulation condition or normal condition, suction valve opening process
$\theta_{s2} - \theta_{s3}$	No	Capacity regulation condition or normal condition, suction process
$\theta_{s3} - \theta_{s4}$	No	Normal condition, suction valve closing process
θ_{s4}	No	Reversal point of piston, i. e. crank angle is 180 °
$\theta_{s3} - \theta_3$	Yes	Capacity regulation condition, suction valve is pressed off, reflux process
$\theta_3 - \theta_4$	No	When $a_v \leqslant a_a$, suction valve closing process
$\theta_{s5} - \theta_4$	Yes	When $a_v \geqslant a_a$, suction valve closing process
θ_3	No	To avoid the impact between unloader and valve plate, unloader is pressed off after suction valve opening process

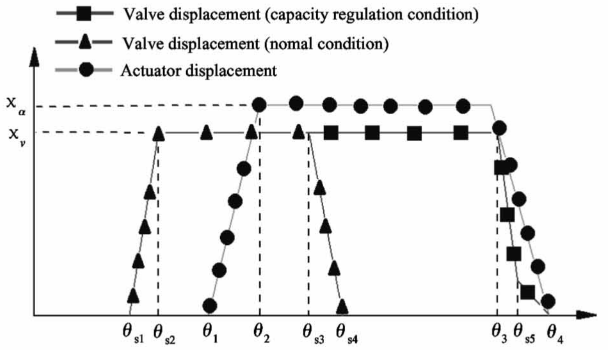

Fig. 2 Displacement diagram of unloader and suction valve

Based on the above analysis, a compressor mathematical model based on capacity control system is established. Before establishing the mathematical model, the following hypothesis is proposed.

(1) The suction valve is an automatic valve, which is not affected by the actuator during the opening process.

(2) The motion of the exhaust valve and suction valve plates is one-dimensional.

(3) The flow of gas through the valve gap is a one-dimensional flow of ideal gas and an adiabatic process.

(4) The cylinder transfers heat with the cooling water in outer wall, which is simulated as an inter-wall heat exchanger, and its heat transfer coefficient is B ($\mathrm{J/(m^2 \cdot s)}$).

1.2.1 Expansion, suction and compression processes

Under capacity control condition, the motion of the actuator doesn't affect the expansion, suction and compression processes[19]. The motion differential equations of the suction valve plate in different processes are respectively:

$$\mathrm{d}p = \frac{kp\,\dfrac{V_h}{2}(\omega\sin(\omega t) + \dfrac{\lambda}{2}\omega\sin(2\omega t))\mathrm{d}\theta + (k-1)C\left(1 - \cos\omega t + \dfrac{\lambda}{2}\sin^2\omega t\right)\mathrm{d}\theta}{-\omega(V_0 + \dfrac{V_h}{2}(1 - \cos(\omega t) + \dfrac{\lambda}{2}\sin^2(\omega t)))} \tag{4}$$

$$\begin{cases} \dfrac{\mathrm{d}h}{\mathrm{d}\theta} = v \\ \dfrac{\mathrm{d}v}{\mathrm{d}\theta} = \dfrac{1}{M_v\omega^2}(\beta p_s(1-\varphi)A_p - ZK(H_0 + h)) \\ \dfrac{\mathrm{d}\varphi}{\mathrm{d}\theta} = -[C(1 - \cos\omega t + \dfrac{\lambda}{2}\sin^2\omega t)\dfrac{k-1}{V_{cy}\omega p_s} + \varphi\dfrac{k\mathrm{d}V_{cy}}{V_{cy}\mathrm{d}\theta} \\ -\dfrac{k}{\omega}(\dfrac{p_{cy}}{p_s})^{(\frac{1}{k})}\alpha_{sv}A_{sv}\sqrt{\dfrac{2k}{k-1}RT_s[1 - (\dfrac{p_{cy}}{p_s})^{(1-\frac{1}{k})}]}] \end{cases} \tag{5}$$

where, h represents valve plate displacement, θ represents crank angle, $\alpha_{sv}A_{sv}$ represents instantaneous effective valve gap area of suction valve, A_p represents area of valve plate, k represents spring stiffness of valve plate, k represents ratio of specific heat of gas, V_{cy} represents cylinder volume, V_0 represents relative clearance volume, β represents coefficient of heat transfer, $C = B2\pi r_{cy}r_{crk}$, r_{crk} represents crank radius, t represents time, H_0 represents precompression of valve plate spring, M_v represents the valve quality, R represents gas constant, T_s represents suction temperature, β represents coefficient of applied force of gas, Z represents number of the spring, p_s represents inlet pressure, p_{cy} represents cylinder pressure, V_h represents stroke volume, λ represents ratio between the crankshaft radius and connecting rod length, r_{cy} represents radius of the cylinder.

Eq. (4) is the motion differential equations of the suction valve plate in the expansion and compression process, and Eq. (5) is the motion differential equations of the suction valve plate in the suction process.

1.2.2 Backflow and suction valve closing process

(1) Backflow process

During the backflow process, the suction valve is forced to open and remain stationary due to the force of the actuator. So $\frac{dv}{d\theta}$ in Eq. (5) is equal to zero. The equation of the backflow process is shown in Eq. (6).

$$\begin{cases} \dfrac{dh}{d\theta} = 0 \\ \dfrac{dv}{d\theta} = 0 \\ \dfrac{d\varphi}{d\theta} = -\Big[C\big(1 - \cos\omega t + \dfrac{\lambda}{2}\sin^2\omega t\big)\dfrac{k-1}{V_{cy}\omega p_s} + \varphi\dfrac{k\mathrm{d}V_{cy}}{V_{cy}\mathrm{d}\theta} \\ \quad - \dfrac{k}{\omega}\Big(\dfrac{p_{cy}}{p_s}\Big)^{(\frac{1}{k})}\alpha_{sv}A_{sv}\sqrt{\dfrac{2k}{k-1}RT_s\Big[1 - \Big(\dfrac{p_{cy}}{p_s}\Big)^{(1-\frac{1}{k})}\Big]}\Big] \end{cases} \quad \theta'_{s4} \leqslant \theta \leqslant \theta_3 \qquad (6)$$

(2) Suction valve closing process

When the withdrawal speed of valve plate is greater than the unloader, the acceleration of the valve plate is equal to the unloading device, so, $\frac{dv}{d\theta}$ in Eq. (7) is equal to Eq. (3). The equation of the suction valve closing process is shown in Eq. (7).

$$\begin{cases} \dfrac{dh}{d\theta} = v \\ \dfrac{dv}{d\theta} = \dfrac{1}{w}\dfrac{F_s - F_h - P + F_i - mg\cos\alpha + \gamma F_{cy}}{m} \\ \dfrac{d\varphi}{d\theta} = -\Big[C\big(1 - \cos\omega t + \dfrac{\lambda}{2}\sin^2\omega t\big)\dfrac{k-1}{V_{cy}\omega p_s} + \varphi\dfrac{k\mathrm{d}V_{cy}}{V_{cy}\mathrm{d}\theta} \\ \quad + \dfrac{k}{\omega V_{cy}}\Big(\dfrac{p_{cy}}{p_s}\Big)^{(1-\frac{1}{k})}\alpha_{sv}A_{sv}\sqrt{\dfrac{2k}{k-1}RT_s\Big[\Big(\dfrac{p_{cy}}{p_s}\Big)^{(1-\frac{1}{k})} - 1\Big]}\Big] \end{cases} \quad \theta_3 \leqslant \theta \leqslant \theta_4 \qquad (7)$$

When the withdrawal speed of valve plate is less than the unloader, the equation is consistent with Eq. (5).

2 Multi-objective optimization mathematical model of actuator based on NSGA-II

2.1 Multi-objective optimization mathematical model

The hydraulic pressure and the reset spring stiffness have great influence on the safety, reliability and performance of the capacity control system. The reduction of hydraulic pressure can decrease the design cost of hydraulic system, decrease the impact of ejection speed and increase the safety of the system, but the actuator can not meet the requirements of ejecting when the hydraulic pressure is small. The decrease of spring stiffness can reduce the design value of hydraulic pressure, but when the spring stiffness decreases, the impact speed of ejection will increase, which is not conducive to system reliability. On the other hand, on account of the valve plate retracts with the actuator, the reduction of spring stiffness will lead to the reduction of the actuator's retract acceleration, so the valve plate closing time increases, the quantity of reflux increases, and the load deviation increases. Therefore, it is necessary to consider the mutual inhibition and contradictory relationship among multiple parameters and objectives, such as hydraulic pressure, spring stiffness, impact velocity of ejection, and regulating effect, as shown in Fig. 3. Based on the mathematical model of actuator and compressor in Section 2, the multi-objective optimization study of load deviation, impact velocity of ejection, hydraulic pressure and spring stiffness is carried out. The multi-objective mathematical model of the unloader is shown in Eqs(8,9):

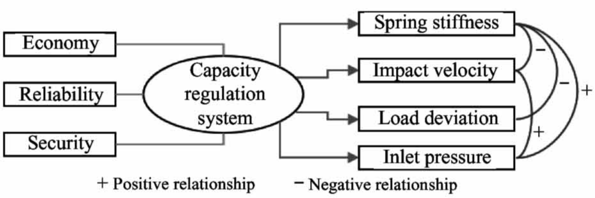

Fig. 3 Parameter relational graph

$$\min f(X) = [f_1 f_2 \cdots f_m] \qquad (8)$$

$$\text{sub } X = (x_1 x_2 \cdots x_n) \\ x_{\text{lower}} \leqslant x_i \leqslant x_{\text{upper}} (i = 1, 2, \cdots, n) \qquad (9)$$

where, $f(X)$ is the objective equation of X; m, n is the number of objective function and decision variables respectively; x_{lower} is the lower limit of the decision variable; x_{upper} is the upper limit of the decision variable.

Therefore, the objective function is to minimize the spring stiffness, oil inlet pressure, impact velocity of ejection and load adjustment deviation. The objective function is described as follows.

(1) Spring stiffness and oil inlet pressure

The design of reducing the system hydraulic pressure and the spring stiffness of unloader can reduce the processing requirements and costs of the actuator and hydraulic system, and increase the safety coefficient of the system.

$$f_1 = k$$

$$f_2 = p_1$$

(2) Load adjustment deviation

Under normal condition, the suction valve plate retracts automatically. Through numerical calculation of Eqs(4) and (5), the withdrawal time of the suction valve plate is 1.56 ms. Actuator parameters are shown in Table 3. Reciprocating compressor parameters are shown in Table 4. Ultimate withdrawal time of unloader is 4 ms with capacity control system. Since the mass of the valve plate is small relative to the unloader, the acceleration of the valve plate is large relative to the unloader. Therefore, under the capacity control condition, the valve plate is withdrawn together with the unloading device, namely, Eq. (7) is adopted as the differential equations of valve plate withdrawal process.

Table 3 Actuator parameters

Parameter	Notation	Unit	Value
Quality of actuator	m	kg	2
Friction	f	N	100
Pre-compression Amount of spring	x_0	m	0.005
Installation angle	α	°	45
Transverse area of plunger	A_{unloader}	m^2	1.1304e-4
Stroke	L	m	0.003
Gas force of suction chamber	F_i	N	0

Table 4 Reciprocating compressor parameters

Parameter	Value	Unit
Crank radius	90	mm
Connecting rod length	450	mm
Diameter of piston rod	45	mm
Diameter of piston	250	mm
Inlet pressure	100	kPa
Exhaust pressure	300	kPa
Total stiffness	8 000	N/m
Ratio of specific heat of gas	1.4	
Crank radius-connecting rod length ratio	0.2	
Valve mass	0.05	kg
Motor speed	500	r/min
Number of similar valves	2	
Suction temperature	27	℃
Discharge temperature	70	℃

Through numerical calculation, the indicated power of compressor with different stiffness is obtained. The load adjustment deviation can be obtained by subtracting the indicated power of the compressor with different stiffness under the normal condition from the indicated power of the compressor under the capacity control condition, that is $\Delta\eta$. The relationship between $\Delta\eta$ and k is obtained as shown in Fig. 4, and through rational fitting, when the numerator degree is 1, denominator degree is 2, fitting degree is high, the relationship between $\Delta\eta$ and k is shown in Eq. (10).

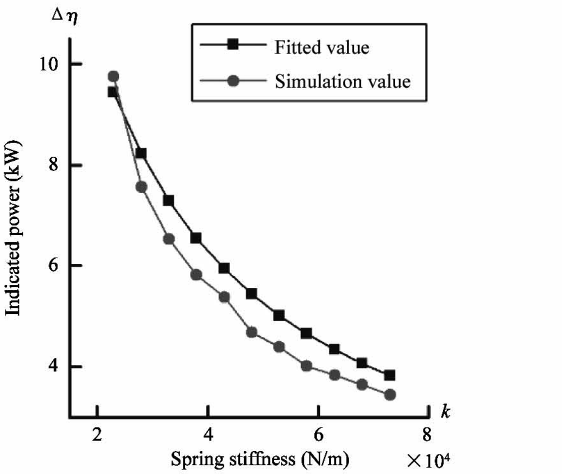

Fig. 4 Fitted curve and simulation curve

$$f_3 = \Delta\eta = \frac{320800k + 4.49}{k^2 + 11020k + 38.8} \tag{10}$$

(3) Impact velocity of ejection

When the angle is $\theta_1 \leqslant \theta \leqslant \theta_2$, it is the ejection process of the actuator, the initial conditions are substituted into the ejection motion differential equation of the actuator, and the velocity at the lower limit of the actuator namely the impact velocity of ejection, can be obtained:

$$f_4 = \nu = -\sqrt{\frac{k}{m}}\left(x_0 - \frac{F_h - F_i - f + mg\cos\alpha}{k_{\text{unloader}}}\right) \sqrt{1 - \left(\frac{L - \dfrac{F_h - F_i - f + mg\cos\alpha}{k_{\text{unloader}}}}{x_0 - \dfrac{F_h - F_i - f + mg\cos\alpha}{k_{\text{unloader}}}}\right)^2} \tag{11}$$

where, $X = (k_{\text{unloader}}, F_h)$ is the decision variable. $\begin{cases} F_h \geqslant F_i + f + F_s(x_0 + L) \\ k_{\text{unloader}} x_0 \geqslant f + mg\cos\alpha \end{cases}$ is the constraint condition.

2.2 Analysis of optimization results based on NSGA-II

Fig. 5 shows the flow of multi-objective optimization algorithm, which is divided into 3 parts. The first part constructs mathematical equations according to the structure and characteristics of the actuator and compressor, the second part analyzes the mutual influence of various parameters and obtains the relational expression according to the mathematical model, and the third part completes the multi-objective optimization calculation with NSGA-II.

The setting parameters of non-dominant sorting multi-objective optimization is shown in Table 5. Figs 6 – 7 show the feasible solution set graph among the 4 targets. As can be seen from Fig. 6, with the decrease of inlet oil pressure or spring stiffness, the impact velocity decreases, but the deviation of indicated power increases. Fig. 6 shows the Pareto front of spring stiffness and oil inlet pressure when Gen = 50, 500, 1 000 and 2 000. As the number of iterations increases, the region of feasible solution gradually decreases and is close to the Pareto front.

Every solution in the NSGA-II solution set is a nondominant solution, and every solution cannot dominate the others. For practical engineering problem of application, the solution of multi-objective problem is not only an optimization problem. When Pareto front is found, the final optimal solution needs to be selected according to the relative importance of the optimization target. Although the deviation of indicated power affects the adjustment accuracy, it can be compensated by the control method. Therefore, the weight of the inlet oil pressure, spring stiffness, impact speed and deviation of indicated power is 0.3 : 0.3 : 0.3 : 0.1. The relationship between r_{ij} and the weight of factors w_i and w_j is $r_{ij} = 0.5 + (w_i - w_j)\beta$, $0 < \beta \leqslant 0.5$, taking $\beta = 0.3$, therefore precedence relation matrix is:

$$\begin{bmatrix} 0.5 & 0.5 & 0.5 & 0.58 \\ 0.5 & 0.5 & 0.5 & 0.58 \\ 0.5 & 0.5 & 0.5 & 0.58 \\ 0.42 & 0.42 & 0.42 & 0.5 \end{bmatrix}$$

Table 5 Parameter of NSGA-II

Parameter	Value
Population size	100
Maximum generation	1 000
Mutation fraction	0.7
Crossover fraction	0.4
Variation ratio	0.02
Crossover ratio	0.02

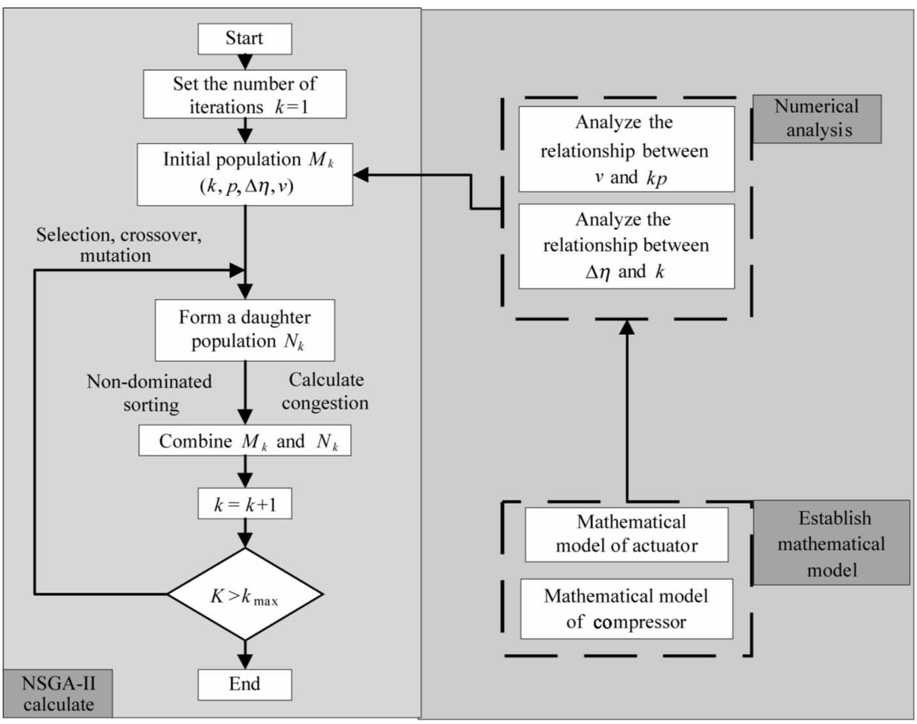

Fig. 5 Multi-objective optimization design algorithm flow chart

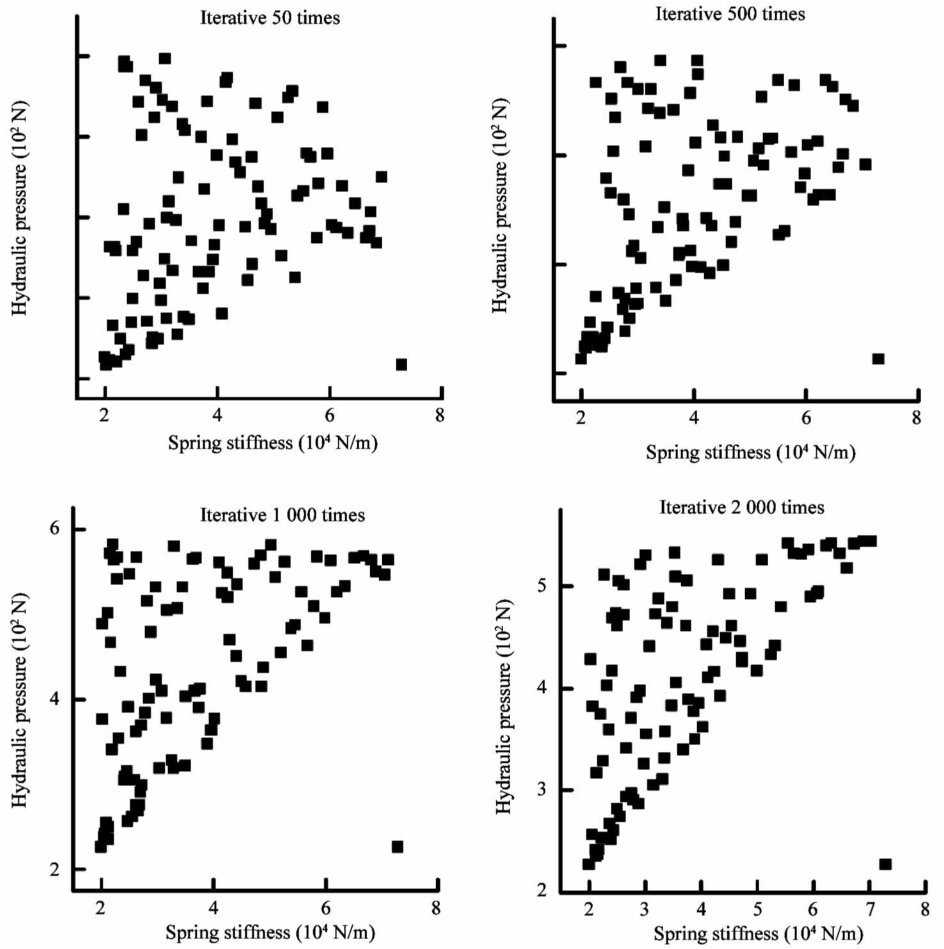

Fig. 6 Spring stiffness and hydraulic pressure Pareto front

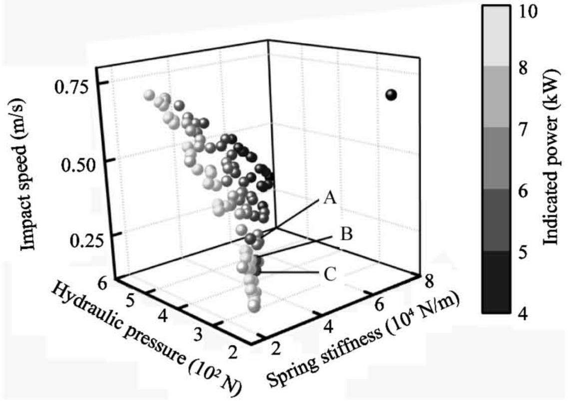

Fig. 7 $k - p_1 - v - \Delta\eta$ Pareto front

Fuzzy consistency matrix is

$$\begin{bmatrix} 0.5 & 0.5 & 0.5 & 0.54 \\ 0.5 & 0.5 & 0.5 & 0.54 \\ 0.5 & 0.5 & 0.5 & 0.54 \\ 0.46 & 0.46 & 0.46 & 0.5 \end{bmatrix}$$

Therefore,

$$W_i = \frac{\sum_{j=1}^{n} r_{ij} + \frac{n}{2} - 1}{n(n-1)} = (0.2533,\ 0.2533,\ 0.2533,\ 0.24)$$

According to the weight coefficient, the optimal solution can be obtained:

$$\min\left(w_1 \frac{k}{k_{\text{range}}} + w_2 \frac{p_1}{p_{1\text{range}}} + w_3 \frac{v}{v_{\text{range}}} + w_4 \frac{\Delta\eta}{\Delta\eta_{\text{range}}}\right)$$

Take the first 3 groups of solutions, as shown in Table 6.

The optimized result of NSGA-II is compared with the traditional design parameters. The traditional design parameters are selected and calculated based on feasibility without considering the optimized design. Therefore, it can be seen from Table 7, the parameters decrease after the optimized design that could reach at least 17% and the maximum could reach 201%.

3 Conclusion

In this work, the key parameters of reciprocating compressor actuator and hydraulic system are optimized

Table 6 Optimal solution of actuator parameters

Index	Spring stiffness	Hydraulic force	Impact velocity	Indicated power difference
A	33 214 N/m	310.63 N	0.2372 m/s	7.2523 kW
B	28 886 N/m	286.43 N	0.2341 m/s	8.0389 kW
C	31 556 N/m	304.96 N	0.2494 m/s	7.5348 kW

Table 7 Optimal solution of actuator parameters

	This paper	Ref. [15]	Ref. [20]	Max decrease	Min decrease
Spring stiffness	33 214 N/m	40 000 N/m	100 000 N/m	201%	17%
Hydraulic force	310.63 N	405.00 N	904.00 N	191%	30%

under capacity control system. Due to the mutual influence of spring stiffness, inlet oil pressure, impact velocity of ejection and deviation of indicated power, the improvement of any parameter will lead to the deterioration of other parameters. In order to solve the multi-parameter optimal design effectively, NSGA-II is used to solve the problem and compared with the traditional results.

(1) The differential equation of actuator motion is established to analyze the relationship between spring stiffness, inlet oil pressure, impact velocity of ejection, which lays a theoretical foundation for multi-objective optimization.

(2) The mathematical model of compressor under the capacity control system is established. On normal condition, the automatic withdrawal time of the valve plate is about 1.56 ms, while the minimum withdrawal time of the unloader on capacity control condition is 4 ms, so the valve plate and the unloader are withdrawn to the top limit together. The motion equation of the valve plate on capacity control system is related to the motion of the actuator. Therefore, the influence of spring stiffness on the indicated power and the displacement of the valve plate is analyzed by combining the motion differential equation of the actuator with the mathematical model of the compressor. The influence of spring stiffness on indicated power and displacement of valve plate on capacity control system is analyzed. It can be seen from the results that with the increase of spring stiffness, the closing time of valve plate decreases and the backflow decreases. Therefore, the deviation of indicated power of capacity control system decreases, but the increase of stiffness will lead to the increase of inlet oil pressure, and the relationship curve between spring stiffness and indicating power deviation is obtained through rational fitting. The above research lays a theoretical foundation for multi-objective optimization.

(3) The optimal design is carried out by using NSGA-II to get Pareto front, and the optimal parameters of actuator and hydraulic system are obtained by adopting fuzzy analytic hierarchy process. The spring stiffness is 33 214 N/m, the inlet oil force is 310.63 N, the impact velocity of ejection is 0.2372 m/s, and the deviation of indicated power is 7.2523 kW. Compared with the traditional design parameters, the optimized design can reduce the spring stiffness or inlet oil pressure by at least 17% and the maximum by 201%.

References

[1] Steinruck P, Ottitsch F, Linskeseder M. Better reciprocating compressor capacity control [J]. *Hydrocarbon Processing*, 1997, 76(2): 79-84

[2] White K H. Infinitely variable capacity control[C] // Proceedings of the Purdue Compressor Technology Conference, Purdue University, USA, 1972:47-51

[3] Almasi A . Reciprocating compressor control[J]. *Process and Control Engineering*, 2013:363-370

[4] Tuymer J W. Stepless variable capacity control[C] // In Proceedings of the International Compressor Engineering Conference, Purdue, USA, 1974:61-66

[5] Steinruck P. Method and apparatus for controlling compressor valves in a piston compressor [P]. US patent: 5988985, 1999

[6] Yao H, Zuo P, Jing Y E. Application of the stepless control system of compressor in continuous reforming unit [J]. *Chemical Engineering and Machinery*, 2016, 43 (1):107-111

[7] Wang Z F, Lou D S. Feng W D. HydroCOM gas capacity stepless regulating system for fresh hydrogen compressor in hydrocracking unit [J]. *Control and Instruments in Chemical Industry*, 2018, 45(12):13-16

[8] Wang B Y, Liu W B, Fang Z. Application of hydroCOM stepless capacity regulating system in reciprocating compressor[J]. *New Technology and New Process*, 2014, 12:109-114

[9] Hong W R, Ye L. The mechanical effects of reciprocating compressor in full-range capacity stepless control system [J]. *Journal of Engineering Thermophysics*, 2011, 32 (1): 49-52

[10] Wang M, Sun X, Zhang J J. Fault simulation and diagnosis of suction valve on reciprocating compressor with sepless capacity control [J]. *Fluid Machinery*, 2019, 47 (4):39-44

[11] Zheng Z X, Jiang Z N, Wang Y Z, et al. Study on the operating characteristics of unloader of reciprocating compressor stepless capacity regulation system[J]. *Journal of Mechanical Strength*, 2019, 41(3):743-747
[12] Heng Z X, Zhao Y X, Meng Y Q, et al. Research of packing seal failure occurred in unloading rod of stepless capacity control system and countermeasures[J]. *Compressor Technology*, 2013,5:66-68
[13] Wu R R, Guan Y H. Regulation device in infinitely variable capacity valve and analysis on optimized regulation force[J]. *Fluid Machinery*, 2005, 33(6):22-25
[14] Li M L, Zhao G Y, Hong W R, et al. Valve plate roll analysis on stepless capacity regulation for reciprocating compressor[J]. *Compressor Technology*, 2013,1:21-23
[15] Cao J L, Li Y. Study of hydraulic actuator performance used in compressor capacity regulation system[J]. *Machine Tool and Hydraulics*, 2015,43(23):35-38
[16] Li Y, Hong W R. Design of pressing-off force in reciprocating compressor capacity regulation[J]. *Compressor Technology*, 2015,1:30-32
[17] Deb K, Pratap A, Agarwal S, et al. A fast and elitist multiobjective genetic algorithm: NSGA-II[J]. *IEEE Transactions on Evolutionary Computation*, 2002, 6(2): 182-197
[18] Jeyadevi S, Baskar S, Babulal C K, et al. Solving multiobjective optimal reactive power dispatch using modified NSGA-II[J]. *International Journal of Electrical Power and Energy Systems*, 2011, 33(2): 219-228
[19] Lin M, Wu Y. Self-acting Valve of Compressors[M]. Xi'an:Xi'an Jiao Tong University Press, 1991 (In Chinese)
[20] Bao B B. Research and Application of Stepless Capacity Control System of Reciprocating Compressor[D]. Beijing: College of Mechanical and Electrical Engineering, Beijing University of Chemical Technology, 2016 (In Chinese)

Zhou Chao, born in 1991. He is currently pursuing his Ph. D degree at Diagnosis and Self-recovery Engineering Research Center of Beijing University of Chemical Technology. He received his B. S. and M. S. degrees from Beijing University of Chemical Technology in 2014 and 2017, respectively. His research interests include stepless capacity control of reciprocating compressor.